

- ¹J. P. Rebouillatt, A. Lienard, J. M. D. Coey, R. Arrese-Bogiano, and J. Chappert, *Physica B+C* **86-88**, 773 (1977); J. M. D. Coey, J. Chappert, J. P. Rebouillatt, and T. S. Wang, *Phys. Rev. Lett.* **36**, 1061 (1976).
- ²R. Harris, M. Plischke, and M. J. Zuckermann, *Phys. Rev. Lett.* **31**, 160 (1973).
- ³D. Sarkar, R. Segnan, E. K. Cornell, E. Callen, R. Harris, M. Plischke, and M. J. Zuckermann, *Phys. Rev. Lett.* **32**, 542 (1974).
- ⁴E. Callen, Y. J. Liu, and J. R. Cullen, *Phys. Rev.* **B16**, 263 (1977); M. C. Chi and R. Alben, *J. Appl. Phys.* **48**, 2987 (1977).
- ⁵P. W. Anderson, B. I. Halperin, and C. H. Varma, *Phil. Mag.* **25**, 1 (1972); J. L. Black and B. I. Halperin, *Phys. Rev.* **B16**, 2879 (1977).
- ⁶W. A. Phillips, *J. Low Temp. Phys.* **7**, 351 (1972).
- ⁷S. A. Al'tshuler and B. M. Kozyrev, *Élektronnyĭ paramagnitnyĭ rezonans (Electron Paramagnetic Resonance)*, Nauka, 1972 [transl., Halsted Press (Wiley), 1975].
- ⁸C. Kittel, *Quantum Theory of Solids*, Wiley, 1963 (Russ. transl., "Nauka", 1967).
- ⁹R. W. Cochrane, R. Harris, and M. Plischke, *J. Non-Cryst. Solids* **15**, 239 (1974).
- ¹⁰R. W. Cochrane, R. Harris, M. Plischke, D. Zobin, and M. J. Zuckermann, *J. Phys. F* **5**, 763 (1975).
- ¹¹A. Aharony, *Phys. Rev.* **B12**, 1038 (1975); J. H. Chen and T. C. Lubensky, *Phys. Rev.* **B16**, 2106 (1977); R. A. Pelcovits, E. Pytte, and J. Rudnick, *Phys. Rev. Lett.* **40**, 476 (1978).

Translated by W. F. Brown, Jr.

Dragging of electrons by sound in metals

N. V. Zavaritskii

Institute of Physics Problems, USSR Academy of Sciences

(Submitted 15 June 1978)

Zh. Eksp. Teor. Fiz. **75**, 1873-1884 (November 1978)

A sound wave attenuating in a metal transfers its momentum to the conduction electrons, thus dragging the electrons. This produces in the sample an acoustoelectric voltage v_{ph} and an acoustomagnetic field H_{ph} if the sound flux occupies respectively the entire or part of the sample cross section. These effects were investigated in tin, aluminum, bismuth, and gallium in the interval 4.2-1.2 K. It is shown that dragging of electrons by sound does not depend on temperature; tin has a giant anisotropy of the acoustoelectric voltage v_{ph} , probably as a result of singularities of the Fermi surface. Nonlinear effects connected with the acoustomagnetic field H_{ph} occur in gallium when the sound intensity is increased.

PACS numbers: 72.50. + b, 72.55. + s

INTRODUCTION

The damping of elastic (acoustic) waves in metals at low temperatures is due mainly to their interaction with the conduction electrons. The energy and momentum of the wave are first transferred to the electrons, and are then dissipated when already in the electron system. In this case the sound drags the conduction electrons. A propagating sound wave excites in a conductor a current and an electric field. The possible existence of this effect was first pointed out by Parmenter,¹ who called it acoustoelectric. Although it soon became clear (see, e.g., Ref. 2) that Parmenter's theoretical calculations were in error, the very existence of electron dragging by the sound was subject to no doubt.

When the wave loses an energy Q as a result of interaction with the conduction electrons, the momentum of the elastic wave Q/u (u is the speed of sound) is transferred to the electrons. As a result, in the simplest case, a current flows in the conductor, given by

$$I = e^* \tau Q / m^* u, \quad (1)$$

where e^* and m^* are the charge and mass of the car-

riers, and τ is the relaxation time in the conduction-electron system. The direction of the current depends on whether the charge carriers are electrons or holes.

If the sample circuit is open, then an electric voltage is produced along the conductor

$$E_{ph} = Q / e^* u N, \quad (2)$$

where N is the charge density. It is seen from (2) that the acoustoelectric voltage is larger the smaller the charge density. This is probably why until recently this effect was investigated only in semiconductors³ or in semimetals.^{4,5} In typical metals the expected effect is too small to be detected by the existing measurement methods.

Indeed, assume that optimal conditions are realized in the experiment, and the voltage produced in the sample is due to absorption of the entire energy of the sound wave. (For this purpose it is necessary that the distance between the sample points between which the voltage $V_{ph} = \int E_{ph} dy$, is measured be so large that the sound wave is completely damped between them.) Then

$$V_{ph} = q/eNu, \quad (3)$$

where q is the sound wave energy flux density. Substituting values typical of metals, we get

$$v_{ph} = V_{ph}q^{-1} \approx 5 \cdot 10^{-10} \text{ V} \cdot \text{W}^{-1} \text{ cm}^2.$$

In experiments usually $q \approx 0.1 \times 10^{-2} \text{ W} \cdot \text{cm}^{-2}$ and consequently $V_{ph} \approx 5 \times 10^{-11} - 5 \times 10^{-15} \text{ V}$. This is the highest estimate of the expected effect, which actually can be even smaller.

A real possibility of investigating the acoustoelectric effect in metals appeared after the recent advent of a new generation of instruments, based on the use of weakly coupled superconductors with sensitivity $10^{-14} - 10^{-15} \text{ V}$ (for example the SKIMP installation⁶).

This article describes experiments that led to observation of the acoustoelectric voltage and acoustomagnetic fields in tin, aluminum, bismuth, and gallium. Data are presented on the measurement of the temperature dependence of the electron dragging by the sound, as well as the results of investigation of the giant anisotropy of the acoustoelectric voltage in tin. We have previously published only preliminary results.⁷

EXPERIMENTAL SETUPS

In all the experiments, the measuring sections (the SKIMP installation and the ultrasound generator) were similar. The joint operation of these elements calls for a number of precautions. The point is that if a parasitic high frequency signal of amplitude 10^{-4} V is applied to the sensitive element of the SKIMP installation, then this installation, as all others of its type, operates outside its rated range. At the same time, to excite an ultrasonic converter the HF signal must have an amplitude on the order of one volt or more. It is therefore necessary to shield the sensitive element

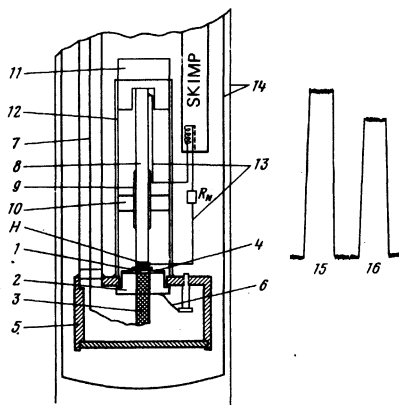


FIG. 1. Instrument for the measurement of the acoustoelectric voltage: 1—acoustic converter, 2—glass insulator with electrode, 3, 4—second electrode of converter—superconducting film, 5—housing of instrument, 6—spring that presses the insulator against the housing, 7—coaxial to feed the converter, 8—sample, 9—remainder of glass mold, 10—guiding washer, 11—weight that clamps the sample to the converter, 12—tube for securing the washers, 13—wires of measuring circuit, 14—lead and Permalloy screens. On the right—typical plot: 15—control signal turned on, 16—HF signal feeding the converter turned on.

very carefully against the HF supply signal of the ultrasound converter. The required shielding is possible only if the entire HF supply line of the converter is in a metallic screen, and that side of the converter which faces the sample is covered with a screening superconductor film (see Fig. 1).

Figure 1 shows a diagram of the instrument used for the measurement of the voltage produced when sound propagates along the sample. The converter of the HF electromagnetic oscillations into acoustic ones was a plate of lithium niobate $\sim 150 \mu\text{m}$ thick. It is known⁸ that the conversion coefficient of lithium niobate reaches 60%. The orientation of the plates for the excitation of various modes was selected in accordance with the data of Korolyuk *et al.*⁹ The measurements were usually performed for the longitudinal (L) oscillation mode at frequencies 23 and 69 MHz and for the transverse (T) mode at 15 and 45 MHz at a power 10^{-3} W dissipated in the radiator. The lithium-niobate plate 1 was secured with epoxy resin to a glass insulator 2 in which an electrode 3 was fused-in. The insulator was fitted snugly into the housing 5. The lithium niobate was covered from above by metallic and superconducting films 4.

The sample 8 (a single crystal cylinder of $\sim 3 \text{ mm}$ diameter) could glide freely in a guiding washer 10, and was pressed against the converter by a weight 11. The lower end of the sample was carefully finished with an electric-spark lathe and was also polished electrically in some experiments. The acoustic contact between the sample and the converter was through a layer of silicone oil. In the measurements of the acoustoelectric effect, the sample was electrically insulated from the converter by a thin layer of BF-2.¹⁾

In the measurements of the voltage, the entire measuring circuit, with the exception of the sample and the "normal" $\sim 3 \times 10^{-8} \Omega$ was connected through superconducting leads. The contact between the leads and the sample was made with Wood's alloy. The voltage V_a produced along the sample when the sound was turned on was measured either with a potentiometer or by determining the direct deflection of the SKIMP installation; a typical waveform obtained by the latter method is shown in Fig. 1.

RESULTS OF MEASUREMENTS AND THEIR DISCUSSION

1. The acoustoelectric effect

In investigations of the acoustoelectric effect, one of the main problems is the separation of the voltage due to the sound wave from the voltage due to the heating of the sample. The heating can be due either to the power dissipated in the converter or to the energy of the damped sound wave. If heating of the sample produces a temperature difference ΔT between the contacts, then the extraneous "thermal" voltage is $V_T = \alpha \Delta T$, where α is the thermoelectric power coefficient of the sample. To separate the acoustoelectric effect from the extraneous thermal effect in the case of tin, we used the fact that the thermoelectric power of pure tin reverses sign in the interval 3.7–4.2 K and passes through zero.¹⁶ It

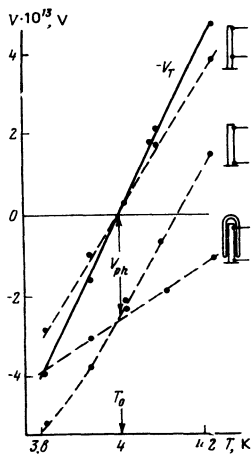


FIG. 2. Temperature dependence of the voltage produced along the sample when the heater on the sample is turned on (solid line) and when the HF signal that feeds the converter is turned on (dashed). The experimental conditions and the location of the contacts are shown schematically on the right of the curves: $\omega = 15$ MHz.

is known that the thermoelectric power coefficient of metals at low temperatures can be represented in the form

$$\alpha = aT + bT^3, \quad (4)$$

where the term aT is due to the direct action of the temperature gradient on the electron system, and bT^3 is due to the action of the phonon wind on the electron system. In the case of tin aT and bT^3 are of opposite sign and become equal at $T = T_0$, where T_0 lies in the interval 3.7–4.2 K. It is clear that at the temperature T_0 at which there is no thermoelectric power in tin the voltage V_A , produced in the sample after turning on the HF signal, is due only to the acoustoelectric effect.

To determine T_0 , a heater H was placed on each sample (Fig. 1). In the first experiment it was located near the contact on the far side of the radiator, but it was found subsequently that it is better to locate it alongside the radiator. The contact was not farther than 0.5 mm from the end face of the sample. Together with the heater it was covered with several layers of paper.

Figure 2 shows the results of one of the first experiments aimed at determining V_{ph} . The heater was located far from the radiator. One of the contacts was placed alongside the heater, and the other at various distances from the radiator, as shown in the figure on the right of the curves. The solid curve is the voltage V_T when the heater H is turned on, and the dashed curve is a plot of V_0 . When the contact is at a considerable distance from the radiator (≈ 1 cm), the sound attenuates before it reaches the contact, and the V_T and V_A curves pass through zero at the same temperature T_0 . On the other hand, if the contact is alongside the radiator, then at $T = T_0$ we have $V_a(T_0) \neq 0$. Obviously, $V_a(T_0) = V_{ph}$ is due to the dragging of the electrons by the sound. The change in the character of the heat transfer from the sample changes dV_a/dT but not V_{ph} . With good approximation, in the entire range of measurements, we have

$$V_a = V_{ph} + \beta V_T. \quad (5)$$

The quantities V_a , V_{ph} , and β are proportional to the square of the voltage of the HF signal on the converter.

A Y-cut converter was used in these experiments, and various sound oscillation modes could be obtained in the same experiment. Figure 3 shows a plot of $V_a(T)$ for the T and L oscillation modes. It is easily seen that the signs of V_{ph} are different for these modes.

The slopes of the dV_T/dT and dV_a/dT curves can be used to determine the sound power flux in the sample, namely,

$$q = Q_H \frac{dV_a}{dT} \left(\frac{dV_T}{dT} S \right)^{-1},$$

where Q_H is the power dissipated in the heater, and S is the cross section area of the sample. This method gives reliable results, of course, only if the heater and the radiator are located at the same contact.

Control experiments have shown that if one sample is used to perform repeated measurements, and the sample is placed in contact each time again with the radiator, the value of V_{ph} can change by several times, whereas the quantity

$$v_{ph} = V_{ph} q^{-1}$$

remains constant. In our estimates, the error in the determination of v_{ph} is of the order of $0.1 v_{ph} \pm 3 \times 10^{-12} \text{ V} \cdot \text{W}^{-1} \text{ cm}^{-2}$. (The second term is connected with the inaccuracy of T_0 .) For the investigated sample we obtained the following values^{7a}:

$$v_{ph, L} = 1.6 \cdot 10^{-11} \text{ W} \cdot \text{W}^{-1} \text{ cm}^2, \quad v_{ph, T} = -2.1 \cdot 10^{-11} \text{ W} \cdot \text{W}^{-1} \text{ cm}^2.$$

The sign of v_{ph} was chosen in accordance with the sign of b in relation (4). A positive sign of v_{ph} means that the acoustoelectric voltage coincides in sign with the voltage due to the phonon wind. The absolute value of v_{ph} of tin turns out to be smaller by one order of magnitude than the previously expected value.

At the same time, for aluminum samples^{7b} we ob-

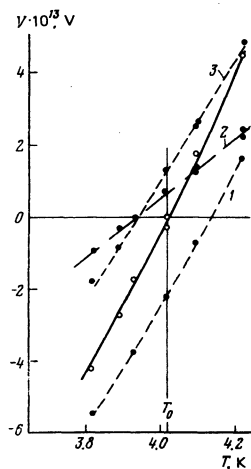


FIG. 3. Temperature dependence of V_a for various oscillation modes: 1— T mode, $\omega = 15$ MHz; 2— L mode, $\omega = 23$ MHz; 3— L mode, $\omega = 69$ MHz; solid curve—for V_T .

served satisfactory agreement between the experimentally determined and calculated values of v_{ph} .

2. Acoustomagnetic effect

The sound wave can excite in metals also a magnetic field. This magnetic field appears if the sound beam occupies only a part of the sample. Then a counter-current of electrons that are not dragged by the sound appears in the sample outside the beam, and the current acquires a circular component and therefore also a magnetic field H_{ph} directed perpendicular to the sound propagation. This effect, called acoustomagnetic, is also a consequence of the dragging of the electrons by the sound. In order of magnitude we have

$$H_{ph} \sim \sigma \eta v_{ph} q,$$

where σ is the conductivity of the metal and η is a geometric factor that depends on the current distribution in the sample. If the sound damping γ is not very large, $\gamma \sim 10$ dB/cm, then $\eta \approx \gamma$. The conductivity of pure metals at helium temperatures is $\sigma \approx 10^{10} \Omega^{-1} \text{ cm}$, and consequently at $\gamma \sim 10$ dB/cm an acoustic flux q of the order of a watt per square centimeter can excite a magnetic field of several oersteds.

It is known¹¹ that a nonequilibrium distribution of the temperature in the sample can lead to the appearance of a magnetic field perpendicular to the temperature gradient only in some exotic cases. Therefore in experiments on the observation of the acoustomagnetic field the role of the extraneous thermal effects is negligibly small, especially if H_{ph} is investigated in the direction of a high-symmetry axis of the crystal.

In our first measurements of the magnetic field we used a movable loop that surrounded a large part of the samples; subsequently we changed over to measurements with a movable loop of area 1 mm^2 , which could be displaced over the surface of the sample in the course of the experiment. The measuring loop together with the receiving coil of the SKIMP installation constituted a single superconducting circuit. In the experiment we measured the current produced in the circuit when the sound was turned on. The installation was calibrated with an additional loop that moved together with the measuring loop and could carry a current of known magnitude. In individual experiments, the same loop was used in the feedback circuit of the SKIMP installation, and H_{ph} was measured by a null method. The samples used in these experiments were single-crystal plates measuring $(8-20) \times 20 \text{ mm}$ and 2 mm thick. A radiator with a construction similar to that described above was located across one of the edges of the plate. The field was measured in the direction perpendicular to $(8-20) \times 20 \text{ mm}$ plane. This direction coincided with the $[001]$ axis in the case of tin, with the C_3 axis in the case of bismuth, and with the c axis in the case of gallium.

It is easily seen that the acoustomagnetic field must be inhomogeneous. The maximum absolute value of the field should be expected near the boundaries of the sound beam, and the field should have opposite directions on opposite sides of the beam. With increasing

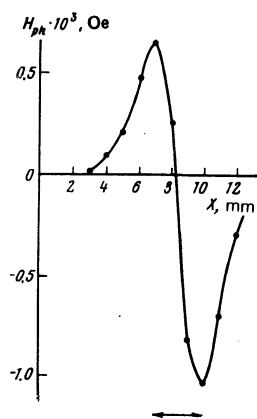


FIG. 4. Section through magnetoacoustic field across the sound beam (X-section); tin, lower arrow-radiator.

distance from the radiator, the field decreases. Some field distortion due to edge effects should be observed near the boundary of the sample.

Figure 4 shows sectional views of the acoustomagnetic field for a tin sample. It is clearly seen that the maximum of H_{ph} indeed coincides with the boundary of the sound beam. The measurements were performed at a distance 3 mm from the radiator, whose dimensions are marked on the figure. No substantial smearing of H_{ph} is noted likewise in the case of measurements at larger distances from the radiator. The value of the field agrees with the estimates based on relation (7). For example, in tin the sound propagated along $[100]$, where $v_{ph} = 5 \times 10^{-11} \text{ V-W}^{-1} \text{ cm}^{-2}$, $\sigma = 3 \times 10^{10} \Omega^{-1} \text{ cm}^{-2}$, $\gamma \sim 20$ dB/cm, and $q = 10^{-2} \text{ W/cm}^2$. Substituting these quantities in (7) we get $H_{ph} \sim 3 \times 10^{-3} \text{ Oe}$, as against the measured $H_{ph} = 10^{-2} \text{ Oe}$.

The value of the acoustomagnetic field at various points of the sample, of course, is determined by the distribution of the sound-induced currents in the sample and can have a more complicated form than shown in Fig. 4. An external magnetic field alters the distribution of the currents and the value of H_{ph} . In weak fields this change reduces mainly to a redistribution of the maxima near the edges of the sound beam (Fig. 5a). In the case of gallium, a substantial redistribution of the field occurs already in fields comparable in magnitude with H_{ph} . The large value of H_{ph} in gallium is a reflection of the high purity of the investigated sample.²⁾ It is clear that in this case the field excited by the ultrasound will alter the distribution of the currents and by the same token influence its own value. These nonlinear effects manifest themselves in the fact that the relative change of H_{ph} over the sample begins to depend on the intensity of the sound flux (Fig. 5b). In this case H_{ph} is no longer proportional to the sound-flux power q (inset in Fig. 5b). In the case of gallium these nonlinear effects set in at $q \approx 2 \times 10^{-2} \text{ W-cm}^{-2}$.

We have demonstrated here only the simplest nonlinear effects due to the large value of H_{ph} . Their actual conceivable variety is large. They are worthy of special consideration, since they can manifest themselves in most unexpected fashion in various experiments with sound. We recall that, for example in experiments on sound absorption, the radiator usually occupies only a

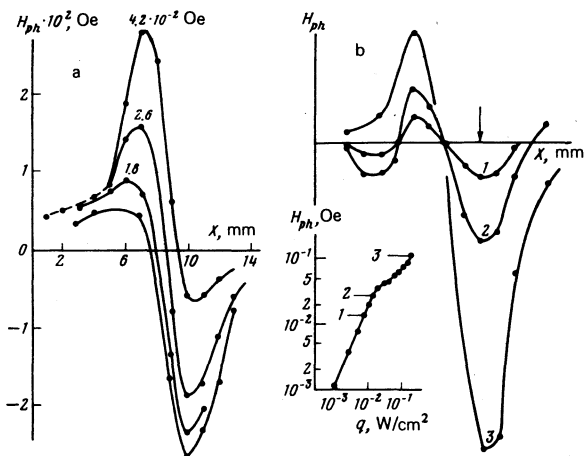


FIG. 5. X-section of magnetoacoustic field in gallium: a— in different external fields (the value of the field is marked on the curve), b—at different sound-beam powers. Inset—dependence of H_{ph} at the maximum, marked by the arrow, on the value of q (the absolute value of q is approximate).

part of the section of the sample. By the same token, in all these experiments there is present an acousto-magnetic field which, in the case of high-purity samples and high sound intensity, can noticeably distort the results of the measurement.

3. Concerning the temperature of the electron dragging by the sound

Although the temperature does not enter directly in the expression (2) for the acoustoelectric effect, one cannot exclude beforehand its possible influence on the dragging of the metal electrons by the sound. Direct measurements of the temperature dependence of v_{ph} in a wide temperature interval is a very complicated task because of the presence of extraneous thermal effects. The experimentally determined relation (5) indicates that in a small temperature interval v_{ph} is constant. To determine the temperature dependence of the electron dragging by the sound in a wider temperature interval

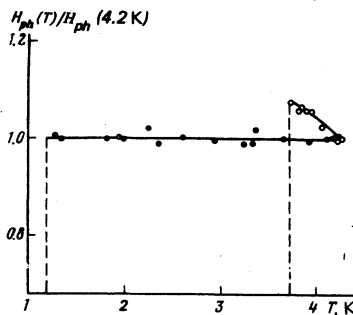


FIG. 7. X-section of magnetoacoustic field in bismuth at various temperatures.

it is convenient to use the acoustomagnetic effect. In this case, however, it must be recognized that even at constant γ the value of H_{ph} depends on the conductivity of the metal.

Figure 6 shows the temperature dependence of H_{ph} in aluminum and tin. In aluminum H_{ph} is constant in the entire measurement interval 4.2–1.2 K, and in tin an increase of H_{ph} by approximately 10% is observed in the interval 4.2–3.7 K and agrees with the increase of the conductivity of the investigated samples.

According to the data of Kopylov and Mezhev–Deglin,¹² the conductivity of the bismuth used by us increases from 4.2 to 1.2 K by almost five times. This can explain fully the substantial increase of H_{ph} of this metal with decreasing temperature (see Fig. 7). It is interesting to note that there is no noticeable difference between the H_{ph} curves plotted above and below the λ point of helium, i.e., under conditions of different thermal regimes of the sample. This result does not confirm the previously obtained conclusion, based on measurement with a stationary loop, that thermal effects play a noticeable role in the formation of H_{ph} in bismuth.

4. Anisotropy of dragging of tin electrons by sound

The substantial difference between the calculated estimate of v_{ph} and the results of its direct measurement in tin is in fact the only patent contradiction between theory and experiment. To cast light on this question, a detailed investigation was made of the anisotropy of the electron dragging by the sound. As described above, the quantity measured in experiment was v_{ph} . The sample orientation was determined by x-ray diffraction accurate to 2°. Samples in the (100) and (001) planes were investigated. If we substitute in (2) the numerical values for tin, we obtain

$$v_{ph,L} = 1.2 \cdot 10^{-10} \text{ V} \cdot \text{W}^{-1} \text{ cm}^2, \quad v_{ph,T} = 2.2 \cdot 10^{-10} \text{ V} \cdot \text{W}^{-1} \text{ cm}^2.$$

In the (100) plane (Fig. 8), for all the directions, the experimental value of v_{ph} is lower by one order of magnitude than expected from the calculations. For most directions, the dependences of $v_{ph,L}$ and $v_{ph,T}$ on the angle are monotonic and similar.³⁾

The picture is different in the (001) plane. The acoustoelectric effect changes quite strongly here (Fig. 9). For example, $v_{ph,L} = 0$ along [100] and [110] whereas at 7–8° away from the [110] direction it approaches the theoretical value. The quantity $v_{ph,T}$ has a different sign and also changes strongly with direction (Fig. 9).

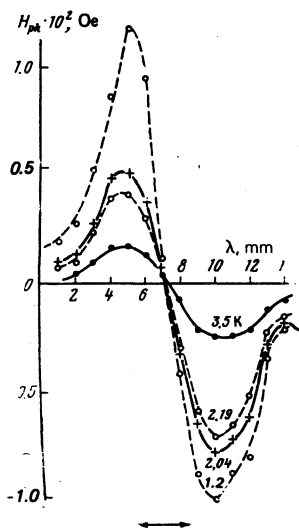


FIG. 6. Temperature dependence of the magnetoacoustic field in aluminum (black points) and tin (light points).

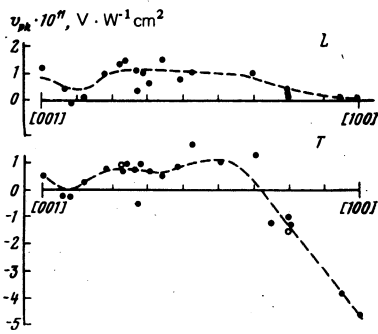


FIG. 8. Acoustoelectric voltage v_{ph} of tin samples of different orientation in the (100) plane.

We can truly speak of a giant anisotropy of the dragging of the tin electrons by the sound in the (001) plane. We recall that this is the plane of the highest crystallographic symmetry in tin. The good agreement between the measurement results obtained with a large number of samples, and the qualitative confirmation of the results in the measurement of the anisotropy of the acoustomagnetic effect on one sample, suggest that the observed change of v_{ph} with changing crystallographic orientation is indeed a property of tin and is not due to random changes in the properties of the samples. We note that measurements at frequencies 15 and 45 MHz lead to close values. A number of typical values of $v_{ph, 45 \text{ MHz}}$ are shown in Figs. 8 and 9 by circles. The maximum difference between v_{15} and v_{45} is observed in the [100] direction and does not exceed 30%. A giant anisotropy of v_{ph} is observed only for samples of extremely high purity. Thus, introduction of approximately 0.01% of bismuth into tin decreases the anisotropy substantially (Fig. 9).

We recall that the anisotropy of the damping of ultrasound is not so large. Thus, according to the data of Perz and Dobbs¹³ a smooth decrease of γ by an approximate factor of four takes place in the (001) plane for the *L* mode when the sound propagation direction changes from [100] to [110].

The acoustoelectric voltage v_{ph} and the thermoelectric power due to the phonon wind are the results of a single physical effect, the dragging of electrons by the sound.

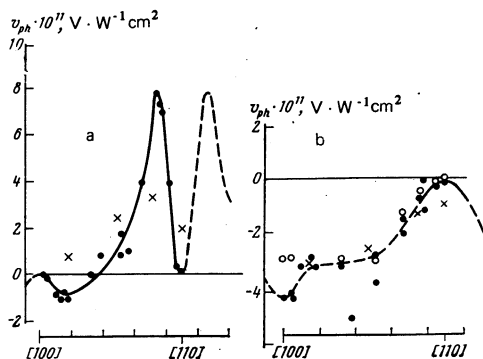


FIG. 9. Acoustoelectric voltage v_{ph} of tin samples of different orientation in (001) plane: a—longitudinal mode, b—transverse mode. Crosses—results of measurements on samples with bismuth impurity.

The only difference is that the frequencies of the sound oscillations (phonons) responsible for these two effects differ by a factor 10^3 . In the case of the thermoelectric power these are oscillations with frequency ~ 100 GHz, and in the acoustoelectric effect these are oscillations with frequency ~ 100 MHz. One can attempt to compare these two effects numerically. To this end, using v_{ph} we calculate the coefficient b in relation (4).

In the presence of a temperature difference ΔT , the phonon flux carries an energy $q \sim cu\Delta T$, where c is the specific heat. At low temperatures $c = c_0 T^3$, where $c_0 = 2.3 \times 10^{-5} \text{ J/cm}^3 \text{ K}^4$ for tin. Substituting the expression for q in (6), we obtain for the voltage due to the phonon wind

$$V_{ph} = v_{ph} c_0 u T^3 \Delta T,$$

from which we get

$$b = c_0 u v_{ph}.$$

In all the relations it is necessary, of course, to substitute the average values of v_{ph} and u . For v_{ph} we use a value encountered for most directions, namely $\sim 10^{-1} \text{ V} \cdot \text{W}^{-1} \text{ cm}^{-2}$, and for the average sound velocity we put $u = 2.5 \times 10^5 \text{ cm} \cdot \text{sec}^{-1}$. This yields $b \sim 1 \times 10^{-10} \text{ V K}^{-4}$. This is smaller by an approximate factor of three or four than the experimentally determined value of b , according to the latest corrected data of Altukhov.¹⁴ This discrepancy can hardly be regarded as substantial, in view of both the approximate character of the entire calculations and of the fact that at the present time v_{ph} is known for only a limited number of crystallographic directions.

In the interpretation of the results on the anisotropy, it must be borne in mind that tin is a metal with a complicated multiband Fermi surface (see Ref. 15, and the pertinent bibliography). In this case all the relations (1)–(3) become more complicated. For example, the sound wave can be absorbed both by electron and hole surfaces. In our experiments $ql \approx 10\text{--}30$ (q is the wave vector, l is the electron mean free path), and it can be assumed that the contribution made to the losses by all the surfaces is additive, i.e., $Q = \sum_i Q_i$, where Q_i are the losses on the i -th surface. It is obvious that the losses on each surface are anisotropic, and since the losses are determined by the interaction between the elastic wave and the electrons on the strip i of the Fermi surface where $\mathbf{q} \cdot \mathbf{v} = 0$ (\mathbf{v} is the electron velocity), it follows that

$$Q_i \sim \oint \frac{|\Lambda|^2 d\varphi}{v^2(\varphi) K(\varphi)},$$

where $|\Lambda|^2$ is a quantity that depends quadratically on the components of the tensor that relates the change of the electron energy with the strain tensor, and $K(\varphi)$ is the Gaussian curvature of the Fermi surface on the strip over which the integration is carried out. The connection between the current and the sound-wave losses in the case of a multiband metal is complicated and, in view of the complexity of the Fermi surface, several explanations can be offered for the anisotropy of v_{ph} .² This obviously calls for additional experimental and theoretical research.

We shall attempt here only to point a way towards an

explanation of the anisotropy of v_{ph} on the basis of most naive representations. Assume that relation (1) is valid for each of the surfaces, and then

$$I = \sum I_i = \sum e_i \tau_i Q_i u^{-1} m_i^{-1}.$$

Naturally, each of the current components I_i depends on the direction of q (by virtue, for example, of the anisotropy of Q_i , τ_i , and m_i). In addition, in the presence of electron and hole surfaces in the metal, the I_i can have opposite signs.

Obviously, the electric voltage due to the elastic wave

$$E_{ph} = I \sigma^{-1} = \sum e_i \tau_i Q_i m_i^{-1} \sigma^{-1} u^{-1}$$

should as a rule be smaller in this case than called for by relation (2), and should have an appreciable anisotropy. In this model, the experimental value of v_{ph} will approach the value calculated from relation (3) if the sound absorption is mainly on surfaces on which the I_i have the same sign.⁴⁾

CONCLUSION

Let us determine the position occupied by the method described in this article for investigating the interaction of the phonon and electron systems relative to the previously existing methods. As already indicated, this method is closest to the method for determining the electron dragging by measuring the thermoelectric power due to the phonon wind. Whereas the thermoelectric power, however, is determined by an integral effect, in our method all the effects are determined by phonons with distinct directions. From this point of view, our method is close to investigations of ultrasound absorption. It is known, however, that ultrasound absorption does not depend on the effective sign of the charge with which the wave interacts, whereas the electron dragging by the sound depends on the sign of the charge. Thus, the principal role for the T mode along [100] is played by holes for bismuth, gallium, and tin and by electrons for aluminum. Owing to the dependence on the sign of the charge, the anisotropy of the effect has a more complicated character compared with the anisotropy of the sound absorption. One can assume that further investigations of dragging of the electrons by sound will yield additional information on the band structure of the electrons of the metal.

When the sound wave propagates in the metal it excites not only an electric voltage but also a magnetic field. In the case of high-purity samples this magnetic field can reach a value large enough to influence the sound absorption via the electron system. By the same

token, the acoustomagnetic field should lead to the appearance of nonlinear effects.

We have considered here only two aspects of the dragging of electrons by sound; further investigations will show the extent to which these and other trends will be helpful.

The author thanks P. L. Kapitza for support and N. A. Nikitin for technical collaboration.

¹⁾ We used in the investigation tin and gallium with $R_{300}/R_{4.2} \approx 6 \cdot 10^4$, aluminum with $R_{300}/R_{4.2} \approx 2 \cdot 10^4$, and bismuth with $R_{300}/R_{4.2} \approx 3 \cdot 10^2$.

²⁾ The high-purity gallium was kindly provided by the Institute of Chemistry of the Siberian Division of the USSR Academy of Sciences.

³⁾ In this plane, mixing of oscillations of different modes does actually take place at oblique orientations.

⁴⁾ It is shown in Ref. 16 that a reversal of the sign of I_i can occur also on one Fermi surface of complex shape.

¹⁾ P. H. Parmenter, Phys. Rev. **89**, 990 (1953).

²⁾ E. I. Blount, Phys. Rev. **114**, 418 (1959).

³⁾ R. Truell *et al.*, Ultrasonic Methods in Solid State Physics, Academic, 1969; Russ. transl., Mir, 1972, p. 243.

⁴⁾ I. Yamada, J. Phys. Soc. Jpn. **20**, 1424 (1965).

⁵⁾ A. P. Korolyuk and V. F. Roi, Pis'ma Zh. Eksp. Teor. Fiz. **17**, 184 (1973) [JETP Lett. **17**, 131 (1973)].

⁶⁾ N. V. Zavaritskiĭ and A. N. Vetchinkin, Prib. Tekh. Eksp. No. 1, 247 (1974).

⁷⁾ N. V. Zavaritskiĭ, Pis'ma Zh. Eksp. Teor. Fiz. (a) **25**, 61; (b) **26**, 44 (1977) [JETP Lett. (a) **25**, 55; (b) **26**, 39 (1977)].

⁸⁾ E. G. Spenser, P. G. Lonzo, and A. A. Ballman, Proc. IEEE **55**, 2074 (1967).

⁹⁾ A. P. Korolyuk, L. Ya. Matsakov, and V. V. Vasil'chenko, Kristallografiya **15**, 1028 (1970) [Sov. Phys. Crystallogr. **15**, 893 (1971)].

¹⁰⁾ N. V. Zavaritskiĭ and A. A. Altukhov, Zh. Eksp. Teor. Fiz. **70**, 1861 (1976) [Sov. Phys. JETP **43**, 969 (1976)].

¹¹⁾ A. T. Samoĭlovich and A. A. Korenblit, Fiz. Tverd. Tela (Leningrad) **3**, 2054 (1961) [Sov. Phys. Solid State **3**, 1494 (1962)].

¹²⁾ V. N. Kopylov and L. P. Mezhev-Deglin, Fiz. Tverd. Tela (Leningrad) **15**, 13 (1973) [Sov. Phys. Solid State **15**, 8 (1973)].

¹³⁾ J. M. Perz and E. R. Dobbs, Proc. R. Soc. London **297**, 408 (1967).

¹⁴⁾ A. A. Altukhov, Yu. Dzhigaev, N. V. Zavaritskiĭ, and I. Suslov, Zh. Eksp. Teor. Fiz. **75**, No. 12 (1978) [Sov. Phys. JETP **48**, No. 12 (1978)].

¹⁵⁾ A. P. Cracknell, The Fermi Surfaces of Metals, eds. Taylor and Francis, London, 1971.

¹⁶⁾ N. V. Zavaritskiĭ, M. I. Kaganov, and Sh. T. Mevlyut, Pis'ma Zh. Eksp. Teor. Fiz. **28**, 223 (1978) [JETP Lett. **28**, 205 (1978)].

Translated by J. G. Adashko